

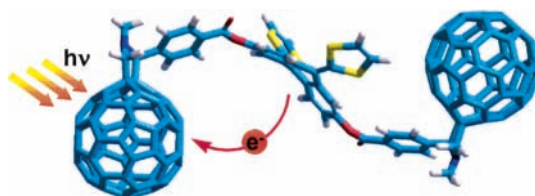
# C<sub>60</sub>–exTTF–C<sub>60</sub> Dumbbells: Cooperative Effects Stemming from Two C<sub>60</sub>s on the Radical Ion Pair Stabilization

Luis Sánchez,<sup>†</sup> María Sierra,<sup>†</sup> Nazario Martín,<sup>\*,†</sup> Dirk M. Guldi,<sup>\*,‡</sup> Martijn W. Wienk,<sup>§</sup> and René A. J. Janssen<sup>\*,§</sup>

Departamento de Química Orgánica, Facultad de Química, Universidad Complutense, E-28040 Madrid, Spain, Institute for Physical Chemistry, Friedrich-Alexander-Universität Erlangen-Nürnberg, Egerlandstr. 3, 91058 Erlangen, Germany, and Chemical Engineering and Chemistry, Eindhoven University of Technology, 5600 MB Eindhoven, The Netherlands  
nazmar@quim.ucm.es; dirk.guldi@chemie.uni-erlangen.de; r.a.j.janssen@tue.nl

Received January 20, 2005

## ABSTRACT



The presence of a second C<sub>60</sub> cage in C<sub>60</sub>–exTTF–C<sub>60</sub> triads [exTTF = 9,10-bis(1,3-dithiol-2-ylidene)-9,10-anthraquinone] has beneficial effects on the stabilization of the radical ion pair formed upon irradiation in comparison with the related C<sub>60</sub>–exTTF dyad. Although C<sub>60</sub>–exTTF–C<sub>60</sub> ensembles show no electronic interaction between the electroactive units in the ground state, their irradiation leads to C<sub>60</sub><sup>•+</sup>–exTTF<sup>•+</sup>–C<sub>60</sub> species with lifetimes on the order of 600 ns in benzonitrile; these lifetimes are twice those determined for the analogous C<sub>60</sub>–exTTF dyad.

The versatile chemistry of C<sub>60</sub>, together with its outstanding electrochemical and photophysical properties, prompted myriad examples of C<sub>60</sub>–donor ensembles. The design of biomimetic model systems, as well as the construction of photovoltaic (PV) devices, is one of the most promising areas.<sup>1</sup>

In contrast to electron–donor fragments such as porphyrins, phthalocyanines, oligomers, or organometallic donors,<sup>2</sup> tetrathiafulvalene (TTF)<sup>3</sup> and its  $\pi$ -extended derivatives (exTTF)<sup>4</sup> gain aromaticity and planarity upon oxidation.<sup>5</sup> These effects have been successfully used to improve significantly the radical ion pair lifetimes formed upon visible light irradiation.

Still the fast charge recombination dynamics, which are

typically seen in most donor–acceptor dyads, diminishes the potential of such architectures for practical applications. A potent approach to overcoming this setback implies the sequential integration of several electroactive fragments. In the corresponding triads, tetrads, etc., larger donor–acceptor

<sup>†</sup> Universidad Complutense.

<sup>‡</sup> Institute for Physical & Theoretical Chemistry.

<sup>§</sup> Eindhoven University of Technology.

(1) (a) Special issue titled *Functionalized Fullerene Materials*: Prato, M.; Martín, N. (Eds.) *J. Mater. Chem.* **2002**, *12*, 1931–2159. (b) *From Synthesis to Optoelectronic Properties*; Guldi, D. M., Martín, N., Eds.; Kluwer Academic Publishers: Dordrecht, The Netherlands, 2002. (c) Guldi, D. M.; Prato, M. *Chem. Commun.* **2004**, 2517–2525.

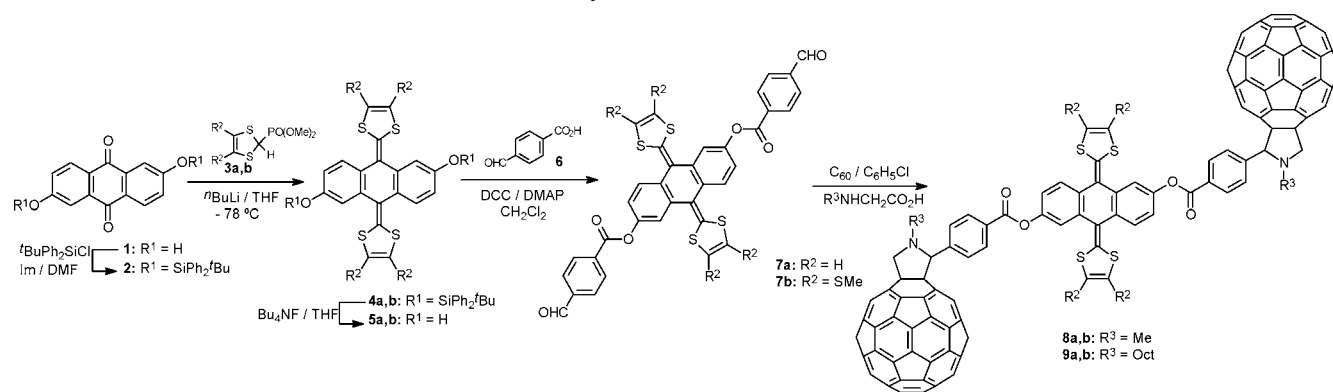
(2) (a) Martín, N.; Sánchez, L.; Illescas, B. Pérez, I. *Chem. Rev.* **1998**, *98*, 2527–2548. (b) Guldi, D. M. *Chem. Soc. Rev.* **2002**, *31*, 22–36. (c) Imahori, H.; Mori, Y.; Matano, Y. *J. Photochem. Photobiol. C* **2003**, *4*, 51–83. (d) Segura, J. L.; Martín, N.; Guldi, D. M. *Chem. Soc. Rev.* **2005**, *34*, 31–47.

(3) (a) Martín, N.; Sánchez, L.; Herranz, M. A.; Guldi, D. M. *J. Phys. Chem. A* **2000**, *104*, 4648–4657. (b) Guldi, D. M.; González, S.; Martín, N.; Antón, A.; Garín, J.; Orduna, J. *J. Org. Chem.* **2000**, *65*, 1978–1983. (c) González, S.; Swartz, A.; Martín, N.; Guldi, D. M. *Org. Lett.* **2003**, *5*, 557–560.

(4) (a) Martín, N.; Pérez, I.; Sánchez, L.; Seoane, C. *J. Org. Chem.* **1997**, *62*, 5690–5695. (b) Herranz, M. A.; Martín, N. *Org. Lett.* **1999**, *1*, 2005–2007. (c) Martín, N.; Sánchez, L.; Guldi, D. M. *Chem. Commun.* **2000**, 113–114. (d) Herranz, M. A.; Martín, N.; Ramey, J.; Guldi, D. M. *Chem. Commun.* **2002**, 2968–2969. (e) González, S.; Martín, N.; Guldi, D. M. *J. Org. Chem.* **2003**, *68*, 779–791. (f) Giacalone, F.; Segura, J. L.; Martín, N.; Guldi, D. M. *J. Am. Chem. Soc.* **2004**, *126*, 5340–5341.

(5) Martín, N.; Sánchez, L.; Seoane, C.; Ortí, E.; Viruela, P. M.; Viruela, R. *J. Org. Chem.* **1998**, *63*, 1268–1279.

# Scheme 1. Synthesis of Triads **8a,b** and **9a,b**



separations and smaller electronic coupling elements in the radical ion pair assist in retarding the charge recombination processes.<sup>6</sup> However, the syntheses of such architectures are far from being trivial and are very tedious.

A very elegant approach to obtaining stable radical pairs has been developed by Fukuzumi and co-workers by preparing donor–acceptor dyads with a careful control over the geometry. They show that very high activation energies for the charge recombination process (ca. 0.23 eV) are responsible for generating largely stabilized charge-separated states (120 s at  $-150^{\circ}\text{C}$ ).<sup>7</sup>

A compelling alternative implies the integration of two  $\text{C}_{60}$ s together with a single-electron donor into dumbbell-like arrays. In several of these dumbbell arrays, benefits (i.e., photophysical as well as PV properties) were seen that evolve from the presence of a second  $\text{C}_{60}$ .<sup>8</sup> However, only a few examples have been reported in which the donors are able to form radical cation species by donating a single electron.<sup>9</sup>

In this communication, we report on the synthesis, electrochemistry, and photophysics of a novel series of  $\text{C}_{60}$ -based dumbbell triads bearing one electron donor (i.e., exTTFs), able to release two electrons at the same oxidation potential value, and two electron acceptors (i.e.,  $\text{C}_{60}$ ). In short, longer lifetimes are observed in the photogenerated radical ion pairs due to the presence of two  $\text{C}_{60}$  units in triads **8**.

The synthesis of target triads **8a,b** and **9a,b** was carried out following a multistep synthetic procedure, starting from the previously reported bisaldehyde-exTTFs **7a,b**.<sup>6a</sup> 1,3-Dipolar cycloaddition reaction of the corresponding azomet-

ine ylide, generated in situ from compound **7** and sarcosine, to [60]fullerene yielded **8a** ( $\text{R} = \text{H}$ ) and **8b** ( $\text{R} = \text{SMe}$ ). To optimize the solubility, a similar strategy was followed to obtain **9a,b**, which bear octyl chains.<sup>10</sup> All the final ensembles were isolated as stable solids in good yields (41–57%) (Scheme 1).

The  $^1\text{H}$  NMR spectra of **8a,b** and **9a,b** showed, besides a series of aromatic signatures, the typical resonances of the pyrrolidine moiety at around 5.1 ppm (d,  $J = 9$  Hz, 1H), 4.1 ppm (d,  $J = 9$  Hz, 1H), and 5.2 ppm (s, 1H). This finding is in good agreement with reports on other fulleropyrrolidines.<sup>4a,11</sup> We and others have noticed a particular broadening of the signal that corresponds to the ortho aromatic protons ( $\delta \sim 8$  ppm). This effect has been assigned to the quadratic effect exerted by the contiguous nitrogen atom.<sup>12</sup>

Only the presence of SMe groups or octyl tails for **8b** and **9a,b**, respectively, has allowed their  $^{13}\text{C}$  NMR spectra to be recorded. A series of signals in the aromatic region indicates the lack of symmetry. In the aliphatic region of the spectra, on the other hand, the resonances corresponding to the  $\text{sp}^2$  carbon of the  $\text{C}_{60}$  cage are seen at  $\delta \approx 80$ , 68, and 66 ppm. For **8b**, additional diagnostic signals at  $\delta$  40 ppm, for the N–Me group, and at  $\delta$  20 ppm, for the SMe groups, are observed (See Supporting Information).

Electronic spectra of triads **8a,b** and **9a,b** display absorption bands at approximately 432 nm, which clearly correspond to the features of  $\pi$ -extended TTF.<sup>5</sup> In room-temperature solutions, the singlet ground-state spectra of these triads provide no evidence for a charge-transfer interaction between the two electroactive moieties.

The electrochemical properties of the novel ensembles were tested by cyclic voltammetric measurements at room temperature. The data are shown in Table 1, together with those for  $\text{C}_{60}$  and 9,10-bis(1,3-dithiol-2-ylidene)-9,10-anthraquinone (exTTF, **10**).<sup>5</sup> **8a,b** and **9a,b** showed four quasireversible reduction waves, which all correspond to

(6) (a) Sánchez, L.; Pérez, I.; Martín, N.; Guldi, D. M. *Chem. Eur. J.* **2003**, *9*, 2457–2468. (b) Marcos-Ramos, A.; Meskers, S. C. J.; van Hal, P. A.; Knol, J.; Hummelen, J. C.; Janssen, R. A. J. *J. Phys. Chem. A* **2003**, *107*, 9269–9283. (c) Nakamura, T.; Fujitsuka, M.; Araki, Y.; Ito, O.; Ikemoto, J.; Takimiya, K.; Aso, Y.; Otsubo, T. *J. Phys. Chem. B* **2004**, *108*, 10700–10710. (d) Liddell, P. A.; Kodis, G.; de la Garza, L.; Moore, A. L.; Moore, T. A.; Gust, D. J. *J. Phys. Chem. B* **2004**, *108*, 10256–10265. (e) Guldi, D. M.; Imahori, H.; Tamaki, K.; Kashiwagi, Y.; Yamada, H.; Sakata, Y.; Fukuzumi, S. *J. Phys. Chem. A* **2004**, *108*, 541–548.

(7) Ohkubo, K.; Kotani, H.; Shao, J.; Ou, Z.; Kadish, K. M.; Li, G.; Pandey, R. K.; Fusitsuka, M.; Ito, O.; Imahori, H.; Fukuzumi, S. *Angew. Chem., Int. Ed.* **2004**, *43*, 853–856 and references therein.

(8) For a recent review on  $\text{C}_{60}$ –D– $\text{C}_{60}$  triads, see: Sánchez, L.; Herranz, M. A.; Martín, N. *J. Mater. Chem.* **2005**, in press.

(9) (a) Segura, J. L.; Martín, N. *Chem. Soc. Rev.* **2000**, *29*, 13–21. (b) Segura, J. L.; Priego, E. M.; Martín, N.; Luo, C.; Guldi, D. M. *Org. Lett.* **2000**, *2*, 4021–4024.

(10) Segura, M.; Sánchez, L.; de Mendoza, J.; Martín, N.; Guldi, D. M. *J. Am. Chem. Soc.* **2003**, *125*, 15093–15100.

(11) (a) Prato, M.; Maggini, M. *Acc. Chem. Res.* **1998**, *31*, 519–526.

(b) Tagmatarchis, N.; Prato, M. *Synlett* **2003**, 768–779.

(12) *NMR Spectroscopy*; Günter, H., Ed.; John Wiley & Sons: New York, 1995; Chapter 7, p 221.

**Table 1.** Redox Potentials of Novel Triads **8a,b** and **9a,b**

compound <sup>a</sup>	$E^1_{\text{red}}$	$E^2_{\text{red}}$	$E^3_{\text{red}}$	$E^4_{\text{red}}$	$E_{\text{ox}}$
<b>8a</b>	−0.60	−0.98	−1.53	−1.96	0.56
<b>8b</b>	−0.59	−0.99	−1.51	−1.97	0.62
<b>9a</b>	−0.61	−1.00	−1.53	−1.98	0.57
<b>9b</b>	−0.60	−1.00	−1.55	−1.98	0.62
C <sub>60</sub>	−0.54	−0.92	−1.38	−1.86	
<b>10</b>					0.48

<sup>a</sup> Experimental conditions: V vs Ag/Ag<sup>+</sup>; 100 mV/s scan rate; ODCB/MeCN (4/1) solvent; Bu<sub>4</sub>NClO<sub>4</sub> (0.1 M) supporting electrolyte; GCE working electrode.

C<sub>60</sub>-centered processes. Although these reduction steps are cathodically shifted in comparison, for example, to the parent C<sub>60</sub>, no electronic interactions between the fragments are deduced from these investigations. Relative to C<sub>60</sub>, increases of the LUMO energy level in the resulting organofullerenes cause these shifts.<sup>13</sup>

The oxidation potentials in **8** and **9** are, however, anodically shifted relative to **10**. This shift is due to the presence of two oxygen atoms at exTTF, which is in agreement with related systems.<sup>6a,14</sup> These data confirm the lack of appreciable interactions between the electroactive units in the ground state.

The next set of experiments is concerned with steady-state and time-resolved emission spectroscopy. In particular, the long-lived fluorescence of C<sub>60</sub> derivatives emerges as a convenient marker for monitoring intramolecular deactivation processes in donor–acceptor ensembles (i.e., energy/electron-transfer reactions). Upon photoexcitation of *N*-methylfullepyrrolidine, used as a reference, a distinct emission spectrum is noted, for which we determined a quantum yield ( $\Phi$ ) of  $6.0 \times 10^{-4}$ .

At room temperature, the steady-state fluorescence of **8a** and **8b** reveals strongly quenched C<sub>60</sub> emission with quantum yields as low as  $10^{-4}$ . Since these experiments were performed upon irradiating into a C<sub>60</sub>-centered transition, where the absorption of the donor is less than 5%, it leaves an increasingly faster deactivation of the C<sub>60</sub> singlet excited state as the only rationale. Gradually changing the solvent polarity from toluene to benzonitrile impacts the extent of emission quenching (See Table S-1 in Supporting Information).

In time-resolved experiments, we determined a fluorescence lifetime of  $1.6 \pm 0.2$  ns for the C<sub>60</sub> reference in deoxygenated toluene solutions. Quite different are the results for **8a** and **8b**. In toluene, for example, the best fits, with a satisfying  $\chi^2$  value of at least 1, were obtained with lifetimes that were on the order of 570 ps for **8a**. Similar results but with faster deactivation kinetics were gathered in THF, dichloromethane, and benzonitrile, which are all solvents of higher polarity.

Considering the above details in concert, steady-state, and time-resolved emission experiments disclose for **8a** and **8b**

a rapid intramolecular deactivation of the photoexcited C<sub>60</sub> chromophore for which we estimate decay dynamics between 570 and 340 ps. No clear assignment can be made as far as the product characterization is concerned. It is interesting to note that attaching two C<sub>60</sub> cores to the exTTF electron donor leads to insignificant changes in the C<sub>60</sub> deactivation relative to the previously reported dyad that carries just one C<sub>60</sub>.<sup>6a</sup>

To complement the fluorescence studies, the photophysics of C<sub>60</sub>, **8a**, and **8b** were probed by means of time-resolved transient absorption spectroscopy. Pump–probe experiments allowed for the characterization of the dynamic processes, which are associated with the generation and the fate of photoexcited states in the novel hybrids. In addition, they helped in shedding light onto the nature of the photoproduct, that is, an excited state or charge-separated state evolving from an intramolecular energy or electron-transfer process, respectively.

Differential absorption spectra of the C<sub>60</sub> reference in deoxygenated dichloromethane are shown in Figure S1 (see Supporting Information). The transient characteristics are a distinct near-infrared absorption peak, which is generally seen in singlet–singlet absorption spectra of C<sub>60</sub> derivatives. The lifetime of the singlet–singlet intermediate state is relatively short, as C<sub>60</sub> and most of its derivatives convert rapidly to the much longer-lived triplet excited state with nearly unit yield. The process is a spin-forbidden intersystem crossing with a high rate of  $5.0 \times 10^8$  s<sup>−1</sup> driven by an efficient spin–orbit coupling. The spectral characteristics of the triplet excited state are maxima at 360 and 700 nm. The triplet transient, derived from photoexcitation of the C<sub>60</sub> reference, shows no appreciable decay on the nanosecond time scale but relaxes on the microsecond time scale.

For **8a** and **8b**, a distinct maximum at 900 nm resembles that seen for the C<sub>60</sub> reference. Again, we assign the new transient absorption to the singlet excited state centered on C<sub>60</sub>, which evolves from the sequence outlined above. However, in contrast to the 1.6 ns lifetime for the C<sub>60</sub> reference, the corresponding transients in **8a** and **8b** were much shorter-lived, decaying with time constants between 300 and 600 ps. The time constants are a good match to the values derived from the emission decay measurements (vide supra). Furthermore, a new absorption grows in with the same time constant. The product is a broadly absorbing species that is spectrally different from the C<sub>60</sub> triplet state. The differential absorption changes disclose a set of new peaks at 660 and 1000 nm (see Figure 1). The visible maxima are ascribed to the one-electron oxidized form of the donor, while a maximum in the near-infrared region at 1000 nm is an excellent match to the one-electron reduced C<sub>60</sub><sup>•−</sup>. We therefore conclude that the radical ion pair is formed via the appreciable C<sub>60</sub> singlet excited-state decay on the nanosecond time scale but relaxes on the microsecond time scale.

Extending our experiments into the nanosecond domain, we were able to determine the lifetime of the charge-separated state. When comparing the lifetimes as a function of solvent polarity, which reflects the energy gap for charge recombination, we see consistently stabilizing effects toward

(13) Echegoyen, L.; Echegoyen, L. E. *Acc. Chem. Res.* **1998**, *31*, 593–601.

(14) González, S.; Martín, N.; Guldi, D. M. *J. Org. Chem.* **2003**, *68*, 779–791.

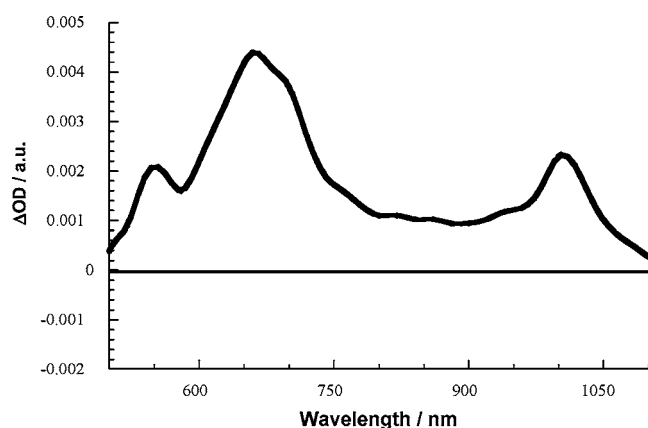


**Figure 1.** Differential absorption spectra (i.e., VIS and NIR) obtained upon nanosecond flash photolysis (355 nm) of **8a** in nitrogen-saturated benzonitrile with a time delay of 50 ns.

the more polar solvents. In fact, this trend suggests that the charge recombination dynamics are in the normal region of the Marcus parabola, that is, the region where the rates decrease with decreasing free energy changes. Much more important is, however, the fact that **8a** and **8b** exhibit radical ion pair lifetimes that are approximately twice as long as those for the corresponding dyad. For example, in benzonitrile the lifetimes are 310 and 630 ns for the dyad **S1** (see Supporting Information) and **8a**, respectively. In other words, linking two  $C_{60}$  cores to exTTF, as an electron donor, leads to better charge delocalization and, consequently, to slower charge recombination.

Preliminary photovoltaic (PV) devices were prepared using a thin layer of compound **9a** as a photoactive material. Glass with PEDOT:PSS-coated ITO was used as a transparent hole collecting electrode and LiF/Al as an electron collecting back

contact. In the dark, a moderate rectification ratio ( $60 \pm 2$  V) is observed, mainly due to an appreciable leakage current. Under illumination with a wolfram halogen lamp ( $75 \text{ mW/cm}^2$ ) a short circuit current density ( $J_{sc}$ ) of  $0.25 \text{ mA/cm}^2$  is obtained together with an open circuit voltage ( $V_{oc}$ ) of 0.32 V and a fill factor (FF) of 0.27 (Figure S2 in Supporting Information). Remarkably, these values are significantly higher than those measured for the related  $C_{60}$ -TTF dyad ( $J_{sc} = 0.074 \text{ mA/cm}^2$ , FF = 0.29,  $V_{oc} = 0.35 \text{ V}$ ) (Figure S3 in Supporting Information).

In summary, a series of new  $C_{60}$ -exTTF- $C_{60}$  dumbbell triads (**8** and **9**) have been synthesized from bisaldehyde **7**. Whereas no electronic interaction in the ground state has been observed by UV-vis and CV experiments, photophysical studies reveal an efficient electron-transfer process giving rise to the corresponding radical pair with a lifetime of up to 630 ns. One of the most remarkable features for these new dumbbell compounds is the cooperative effect stemming from the presence of a second  $C_{60}$  cage, which, in turn, doubles the lifetime of the corresponding charge-separated state in comparison to the analogous dyad.

**Acknowledgment.** This work has been supported by the MCyT of Spain, Comunidad de Madrid (Projects BQU2002-00855 and HSE/MAT0633-04), the Dutch Polymer Institute (DPI#324), SFB 583, Fond der Chemischen Industrie, and the Office of Basic Energy Science of the U.S. Department of Energy. This is contribution No. NDRL-4597 from the Notre Dame Radiation Laboratory.

**Supporting Information Available:** Experimental details, spectroscopic characterization of all new compounds, and Table S-1 bearing the photophysical features of triad **8** and dyad **S1** in different solvents. This material is available free of charge via the Internet at <http://pubs.acs.org>.

OL050127Z